AEROSPACE REPORT NO.
TOR-0090(5013-01)-1

(4)

AD-A220 204

Expansion Into Vacuum of Gas Bound by Shell and Porous Medium

Prepared by

H. MIRELS
Aerophysics Laboratory
Laboratory Operations

15 February 1990

Prepared for

SPACE SYSTEMS DIVISION
AIR FORCE SYSTEMS COMMAND
Los Angeles Air Force Base
P. O. Box 92960
Los Angeles, CA 90009-2960

Programs Group
THE AEROSPACE CORPORATION

APPROVED FOR PUBLIC RELEASE;
DISTRIBUTION UNLIMITED

LABORATORY OPERATIONS

The Aerospace Corporation functions as an "architect-engineer" for national security projects, specializing in advanced military space systems. Providing research support, the corporation's Laboratory Operations conducts experimental and theoretical investigations that focus on the application of scientific and technical advances to such systems. Vital to the success of these investigations is the technical staff's wide-ranging expertise and its ability to stay current with new developments. This expertise is enhanced by a research program aimed at dealing with the many problems associated with rapidly evolving space systems. Contributing their capabilities to the research effort are these individual laboratories:

Aerophysics Laboratory: Launch vehicle and reentry fluid mechanics, heat transfer and flight dynamics; chemical and electric propulsion, propellant chemistry, chemical dynamics, environmental chemistry, trace detection; spacecraft structural mechanics, contamination, thermal and structural control; high temperature thermomechanics, gas kinetics and radiation; cw and pulsed chemical and excimer laser development, including chemical kinetics, spectroscopy, optical resonators, beam control, atmospheric propagation, laser effects and countermeasures.

Chemistry and Physics Laboratory: Atmospheric chemical reactions, atmospheric optics, light scattering, state-specific chemical reactions and radiative signatures of missile plumes, sensor out-of-field-of-view rejection, applied laser spectroscopy, laser chemistry, laser optoelectronics, solar cell physics, battery electrochemistry, space vacuum and radiation effects on materials, lubrication and surface phenomena, thermionic emission, photosensitive materials and detectors, atomic frequency standards, and environmental chemistry.

Electronics Research Laboratory: Microelectronics, solid-state device physics, compound semiconductors, radiation hardening; electro-optics, quantum electronics, solid-state lasers, optical propagation and communications; microwave semiconductor devices, microwave/millimeter wave measurements, diagnostics and radiometry, microwave/millimeter wave thermionic devices; atomic time and frequency standards; antennas, rf systems, electromagnetic propagation phenomena, space communication systems.

Materials Sciences Laboratory: Development of new materials: metals, alloys, ceramics, polymers and their composites, and new forms of carbon; nondestructive evaluation, component failure analysis and reliability; fracture mechanics and stress corrosion; analysis and evaluation of materials at cryogenic and elevated temperatures as well as in space and enemy-induced environments.

Space Sciences Laboratory: Magnetospheric, auroral and cosmic ray physics, wave-particle interactions, magnetospheric plasma waves; atmospheric and ionospheric physics, density and composition of the upper atmosphere, remote sensing using atmospheric radiation; solar physics, infrared astronomy, infrared signature analysis; effects of solar activity, magnetic storms and nuclear explosions on the earth's atmosphere, ionosphere and magnetosphere; effects of electromagnetic and particulate radiations on space systems; space instrumentation.

Aerospace Report No.
TOR-0090(5013-01)-1

EXPANSION INTO VACUUM OF GAS BOUND BY SHELL AND POROUS MEDIUM

Prepared by

H. Mirels
Aerophysics Laboratory
Laboratory Operations

15 February 1990

Programs Group
THE AEROSPACE CORPORATION
El Segundo, CA 90245-4691

Prepared for

SPACE SYSTEMS DIVISION
AIR FORCE SYSTEMS COMMAND
Los Angeles Air Force Base
P.O. Box 92960
Los Angeles, CA 90009-2960

UNCLASSIFIED

SECURITY CLASSIFICATION OF THIS PAGE

REPORT DOCUMENTATION PAGE

1a. REPORT SECURITY CLASSIFICATION Unclassified	1b. RESTRICTIVE MARKINGS
2a. SECURITY CLASSIFICATION AUTHORITY	3. DISTRIBUTION/AVAILABILITY OF REPORT Approved for public release; distribution unlimited.
2b. DECLASSIFICATION/DOWNGRADING SCHEDULE	
4. PERFORMING ORGANIZATION REPORT NUMBER(S) TOR-0090(5013-01)-1	5. MONITORING ORGANIZATION REPORT NUMBER(S)
6a. NAME OF PERFORMING ORGANIZATION The Aerospace Corporation Laboratory Operations	6b. OFFICE SYMBOL *(If applicable)*
7a. NAME OF MONITORING ORGANIZATION Space Systems Division	
6c. ADDRESS *(City, State, and ZIP Code)* El Segundo, CA 90245-4691	7b. ADDRESS *(City, State, and ZIP Code)* Los Angeles Air Force Base Los Angeles, CA 90009-2960
8a. NAME OF FUNDING/SPONSORING ORGANIZATION	8b. OFFICE SYMBOL *(If applicable)*
9. PROCUREMENT INSTRUMENT IDENTIFICATION NUMBER F04701-88-C-0089	
8c. ADDRESS *(City, State, and ZIP Code)*	10. SOURCE OF FUNDING NUMBERS

PROGRAM ELEMENT NO.	PROJECT NO.	TASK NO.	WORK UNIT ACCESSION NO.

11. TITLE *(Include Security Classification)*
EXPANSION INTO VACUUM OF GAS BOUND BY SHELL AND POROUS MEDIUM

12. PERSONAL AUTHOR(S)
Mirels, H.

13a. TYPE OF REPORT	13b. TIME COVERED	14. DATE OF REPORT *(Year, Month, Day)*	15. PAGE COUNT
	FROM ________ TO ________		

16. SUPPLEMENTARY NOTATION-

17. COSATI CODES			18. SUBJECT TERMS *(Continue on reverse if necessary and identify by block number)*
FIELD	GROUP	SUB-GROUP	

19. ABSTRACT *(Continue on reverse if necessary and identify by block number)*

The expansion into a vacuum of a gas, bound by a shell-like mass with zero tension, has been evaluated. Planar, cylindrical and spherical expansions are considered. The flow is self-similar. The effect of the shell is to reduce expansion velocities, increase gas static pressure, reduce gas dynamic pressure and increase the net impulse at a station. The present study represents a generalization of the Sedov similarity solution for an unbound gas expansion into a vacuum. An approximate local similarity solution is given for the case where the shell is bound by a highly compressible porous medium. After long times, the net momentum of the effective shell continues to increase with increase in radius. The latter result differs from the Zeldovich and Raizer treatment of a point explosion in a porous medium due to inclusion in the present study of the effect of gas pressure on late time shell motion.

20. DISTRIBUTION/AVAILABILITY OF ABSTRACT ☒ UNCLASSIFIED/UNLIMITED ☐ SAME AS RPT. ☐ DTIC USERS	21. ABSTRACT SECURITY CLASSIFICATION Unclassified
22a. NAME OF RESPONSIBLE INDIVIDUAL	22b. TELEPHONE *(Include Area Code)* / 22c. OFFICE SYMBOL

Report No.
TOR-0090(5013-01)-1

EXPANSION INTO VACUUM OF GAS BOUND
BY SHELL AND POROUS MEDIUM

Prepared by

H. Mirels, Principal Scientist
Aerophysics Laboratory

Approved by

W. P. Thompson, Director
Aerophysics Laboratory
Laboratory Operations

L. T. Greenberg, Principal Director
Surveillance and Defense Integration
Programs Group

CONTENTS

FIGURES

TABLES

I. INTRODUCTION

The self-similar solution for the expansion of a gas into a vacuum is well known.[1] In the present study the latter similarity solution is generalized to include cases where the gas is bound by a shell with negligible tensile strength. The shell is assumed to envelop the gas during the entire expansion process. An exact solution is obtained in quadrature form. Analytic expressions for dependent variables are presented for limiting cases.

An approximate local similarity solution is also presented which includes the effect of a highly compressible porous medium external to the shell. The latter solution is compared with the solution by Zeldovich and Raizer of a point explosion in a porous medium.[2]

II. THEORY

We consider the planar ($\sigma = 0$), cylindrical ($\sigma = 1$) and spherical ($\sigma = 2$) case of a gas bound by a shell-like mass which is surrounded by a vacuum (Fig. 1). The expansion is assumed to start at time $t = 0$. The initial gas radius is denoted r_0 and the corresponding shell location is denoted R_0. The initial gas conditions at $r = 0$ are also denoted by subscript zero. We assume that the entropy of the gas is everywhere the same. An exact similarity solution is first obtained. An approximate local similarity solution which includes the effect of a porous medium external to the shell is then indicated.

A. EXACT SIMILARITY SOLUTION

The equations of motion for the gas are

$$\frac{\partial \rho}{\partial t} + \frac{\partial \rho v}{\partial r} + \frac{\sigma \rho v}{r} = 0 \qquad \text{CONTINUITY} \qquad (1a)$$

$$\frac{\partial v}{\partial t} + v\frac{\partial v}{\partial r} = -\frac{\gamma p_0}{\rho_0^{\gamma}}\rho^{\gamma-2}\frac{\partial \rho}{\partial r} \qquad \text{MOMENTUM} \qquad (1b)$$

where $p/\rho^{\gamma} = p_0/\rho_0^{\gamma}$. Symbols are defined in Appendix A. The location of the shell at each instant is denoted $R(t)$. We introduce the similarity variable

$$\eta = r/R \qquad (2)$$

so that the gas is confined to the region $-1 \le \eta \le 1$ for the planar case and to the region $0 \le \eta \le 1$ for $\sigma = 1, 2$. The dependent variables are expressed in the form

$$\frac{\rho}{\rho_0} = \left(\frac{R}{R_0}\right)^{-(\sigma+1)} f(\eta) \qquad (3a)$$

$$v = \dot{R}\eta \qquad (3b)$$

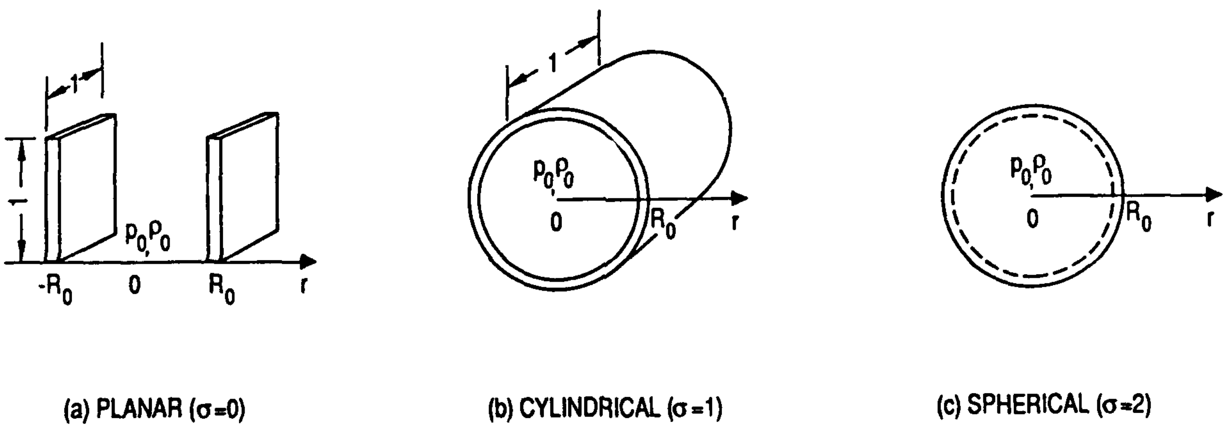

Fig. 1. Initial Conditions for Gas Bound by Shell

which satisfies Eq. (1a). Here, $\dot{R} = dR/dt$. Substitution into Eq. (1b) yields

$$\frac{-R\ \ddot{R}}{a_0^2 (R/R_0)^{-(\gamma-1)(\sigma+1)}} = \frac{f^{\gamma-2}\ df/d\eta}{\eta} = \frac{-2C}{\gamma-1} \tag{4}$$

where C is a constant. Integration of Eq. (4) yields

$$\frac{\rho}{\rho_0} = \left(\frac{p}{p_0}\right)^{1/\gamma} = \left(\frac{R}{R_0}\right)^{-(\sigma+1)} (1-C\eta^2)^{1/(\gamma-1)} \tag{5a}$$

$$\frac{\dot{R}}{\dot{R}_\infty} = \left[1 - \left(\frac{R}{R_0}\right)^{-(\gamma-1)(\sigma+1)}\right]^{1/2} \tag{5b}$$

where $\dot{R}_\infty$ is the speed of the shell after long times and equals

$$\frac{\dot{R}_\infty}{a_0} = \frac{2}{\gamma-1} \left(\frac{C}{\sigma+1}\right)^{1/2} \tag{5c}$$

It is assumed, in Eq. (5b), that $\dot{R} = 0$ at $t = 0$.

The constant C is evaluated by considering the boundary conditions at $\eta = 1$. The total mass of the shell is denoted M_s. The shell mass, per unit area, during the expansion is

$$\frac{\text{SHELL MASS}}{\text{AREA}} = \frac{M_s}{\delta R^\sigma}$$

where $\delta = 2$, 2π and 4π for $\sigma = 0$, 1 and 2. Note that gas volume is given by $\delta R^{\sigma+1}/(\sigma+1)$. The shell is accelerated due to the gas pressure at $\eta = 1$. The appropriate form for Newton's law, at $\eta = 1$, is

$$\delta R^\sigma p_s = M_s\ \ddot{R} \tag{6}$$

where p_s is the gas pressure at $\eta = 1$. The value of C, which is consistent with Eqs. (5) and (6), is

$$C = \frac{\gamma-1}{2\gamma} \frac{\delta R_0^{\sigma+1} \rho_0}{M_s} (1-C)^{\gamma/(\gamma-1)} \tag{7}$$

The quantities ρ_0 and p_0 can be related to the net gas mass M_g and the net initial gas energy E_g via the expressions

$$MI \equiv \frac{(\sigma+1)M_g}{\delta \rho_0 R_0^{\sigma+1}} = (\sigma+1) \int_0^1 (1-C\eta^2)^{1/(\gamma-1)} \eta^\sigma d\eta \tag{8a}$$

$$EI \equiv \frac{(\sigma+1)(\gamma-1)\ E_g}{\delta p_0 R_0^{\sigma+1}} = (\sigma+1) \int_0^1 (1-C\eta^2)^{\gamma/(\gamma-1)} \eta^\sigma d\eta \tag{8b}$$

Note that MI equals the ratio of the average gas density at $t = 0$ to ρ_0. Similarly, EI equals the average gas energy per unit volume at $t = 0$ to the initial energy per unit volume at the origin, $p_0/(\gamma-1)$. Equation (7) can then be expressed

$$\frac{M_g}{M_s} = \frac{2\gamma}{\gamma-1} \frac{MI}{\sigma+1} \frac{C}{(1-C)^{\gamma/(\gamma-1)}} \tag{8c}$$

which relates M_g/M_s to C for a given gas and geometry. Numerical values of MI, EI and M_g/M_s are listed in Table 1 as functions of γ, σ, C. Hence, Eqs. (3) and (5) can be evaluated if γ, σ, and M_g/M_s are specified. It is seen that $0 \leq C \leq 1$ for $0 \leq M_g/M_s \leq \infty$. The case $C = 1$ corresponds to an unbound gas.

Analytic expressions for MI and EI are, respectively,

$$MI = 1 - \frac{\sigma+1}{\sigma+3} \frac{C}{\gamma-1} + \frac{\sigma+1}{\sigma+5} \frac{2-\gamma}{2(\gamma-1)^2} C^2 + 0\ (C^3) \tag{9a}$$

Table 1. Variation of Mass Ratio M_g/M_s, Normalized Mass Integral MI and Normalized Energy Integral EI with $11/9 \le \gamma \le 5/3$, $\sigma = 0,1,2$ and $0.00 \le C \le 1.00$

		SIGMA=0.0			SIGMA=1.0			SIGMA=2.0		
GAMMA	C	MG/MS	MI	EI	MG/MS	MI	EI	MG/MS	MI	EI
1.667	0.00	0.000E+00	1.0000	1.0000	0.000E+00	1.0000	1.0000	0.000E+00	1.0000	1.0000
	0.02	0.104E+00	0.9900	0.9835	0.518E-01	0.9851	0.9753	0.344E-01	0.9821	0.9703
	0.04	0.217E+00	0.9801	0.9673	0.107E+00	0.9702	0.9510	0.712E-01	0.9643	0.9413
	0.06	0.340E+00	0.9703	0.9513	0.167E+00	0.9555	0.9272	0.110E+00	0.9466	0.9129
	0.08	0.473E+00	0.9605	0.9357	0.232E+00	0.9408	0.9040	0.153E+00	0.9290	0.8851
	0.10	0.619E+00	0.9508	0.9204	0.301E+00	0.9263	0.8812	0.198E+00	0.9116	0.8579
	0.20	0.158E+01	0.9031	0.8480	0.747E+00	0.8551	0.7744	0.481E+00	0.8266	0.7313
	0.30	0.314E+01	0.8570	0.7825	0.144E+01	0.7867	0.6791	0.909E+00	0.7451	0.6194
	0.40	0.583E+01	0.8127	0.7237	0.259E+01	0.7212	0.5948	0.160E+01	0.6673	0.5216
	0.50	0.109E+02	0.7701	0.6712	0.466E+01	0.6586	0.5209	0.280E+01	0.5933	0.4371
	0.60	0.216E+02	0.7294	0.6247	0.888E+01	0.5992	0.4569	0.517E+01	0.5235	0.3651
	0.70	0.490E+02	0.6907	0.5838	0.193E+02	0.5433	0.4021	0.108E+02	0.4582	0.3048
	0.80	0.146E+03	0.6543	0.5482	0.549E+02	0.4911	0.3559	0.296E+02	0.3977	0.2553
	0.90	0.882E+03	0.6202	0.5174	0.315E+03	0.4431	0.3174	0.163E+03	0.3428	0.2154
	1.00	INFINITY	0.5891	0.4909	INFINITY	0.4000	0.2857	INFINITY	0.2945	0.1841
GAMMA	C	MG/MS	MI	EI	MG/MS	MI	EI	MG/MS	MI	EI
1.400	0.00	0.000E+00	1.0000	1.0000	0.000E+00	1.0000	1.0000	0.000E+00	1.0000	1.0000
	0.02	0.148E+00	0.9835	0.9770	0.733E-01	0.9752	0.9656	0.486E-01	0.9703	0.9587
	0.04	0.312E+00	0.9673	0.9547	0.154E+00	0.9510	0.9323	0.101E+00	0.9413	0.9190
	0.06	0.496E+00	0.9513	0.9331	0.242E+00	0.9272	0.9001	0.159E+00	0.9129	0.8806
	0.08	0.702E+00	0.9357	0.9121	0.339E+00	0.9040	0.8691	0.221E+00	0.8851	0.8436
	0.10	0.932E+00	0.9204	0.8918	0.446E+00	0.8812	0.8390	0.289E+00	0.8579	0.8080
	0.20	0.259E+01	0.8480	0.7992	0.118E+01	0.7744	0.7040	0.745E+00	0.7313	0.6493
	0.30	0.573E+01	0.7825	0.7206	0.248E+01	0.6791	0.5919	0.151E+01	0.6194	0.5197
	0.40	0.121E+02	0.7237	0.6541	0.498E+01	0.5948	0.4998	0.291E+01	0.5216	0.4153
	0.50	0.266E+02	0.6712	0.5983	0.103E+02	0.5209	0.4248	0.577E+01	0.4371	0.3325
	0.60	0.648E+02	0.6247	0.5517	0.237E+02	0.4569	0.3644	0.126E+02	0.3651	0.2677
	0.70	0.193E+03	0.5838	0.5127	0.666E+02	0.4021	0.3161	0.337E+02	0.3048	0.2178
	0.80	0.858E+03	0.5482	0.4801	0.279E+03	0.3559	0.2776	0.133E+03	0.2553	0.1798
	0.90	0.103E+05	0.5174	0.4527	0.316E+04	0.3174	0.2469	0.143E+04	0.2154	0.1509
	1.00	INFINITY	0.4909	0.4295	INFINITY	0.2857	0.2222	INFINITY	0.1841	0.1289
GAMMA	C	MG/MS	MI	EI	MG/MS	MI	EI	MG/MS	MI	EI
1.286	0.00	0.000E+00	1.0000	1.0000	0.000E+00	1.0000	1.0000	0.000E+00	1.0000	1.0000
	0.02	0.193E+00	0.9770	0.9706	0.952E-01	0.9656	0.9560	0.630E-01	0.9587	0.9473
	0.04	0.413E+00	0.9547	0.9425	0.202E+00	0.9323	0.9141	0.133E+00	0.9189	0.8973
	0.06	0.666E+00	0.9331	0.9155	0.321E+00	0.9001	0.8741	0.209E+00	0.8806	0.8497
	0.08	0.956E+00	0.9121	0.8896	0.455E+00	0.8690	0.8360	0.295E+00	0.8436	0.8045
	0.10	0.129E+01	0.8918	0.8648	0.607E+00	0.8390	0.7997	0.389E+00	0.8080	0.7616
	0.20	0.393E+01	0.7992	0.7559	0.173E+01	0.7040	0.6426	0.106E+01	0.6493	0.5785
	0.30	0.969E+01	0.7206	0.6686	0.398E+01	0.5919	0.5208	0.233E+01	0.5197	0.4400
	0.40	0.235E+02	0.6541	0.5988	0.896E+01	0.4998	0.4272	0.496E+01	0.4153	0.3366
	0.50	0.609E+02	0.5983	0.5429	0.216E+02	0.4248	0.3556	0.113E+02	0.3325	0.2604
	0.60	0.184E+03	0.5517	0.4981	0.608E+02	0.3644	0.3011	0.298E+02	0.2677	0.2048
	0.70	0.728E+03	0.5127	0.4619	0.224E+03	0.3160	0.2594	0.103E+03	0.2178	0.1645
	0.80	0.483E+04	0.4801	0.4322	0.140E+04	0.2776	0.2272	0.603E+03	0.1798	0.1350
	0.90	0.116E+06	0.4527	0.4075	0.316E+05	0.2469	0.2020	0.129E+05	0.1509	0.1132
	1.00	INFINITY	0.4295	0.3866	INFINITY	0.2222	0.1818	INFINITY	0.1288	0.0966
GAMMA	C	MG/MS	MI	EI	MG/MS	MI	EI	MG/MS	MI	EI
1.222	0.00	0.000E+00	1.0000	1.0000	0.000E+00	1.0000	1.0000	0.000E+00	1.0000	1.0000
	0.02	0.239E+00	0.9706	0.9643	0.118E+00	0.9560	0.9466	0.776E-01	0.9473	0.9361
	0.04	0.519E+00	0.9425	0.9305	0.252E+00	0.9141	0.8964	0.165E+00	0.8973	0.8762
	0.06	0.849E+00	0.9155	0.8985	0.405E+00	0.8741	0.8491	0.263E+00	0.8497	0.8201
	0.08	0.124E+01	0.8896	0.8681	0.582E+00	0.8360	0.8046	0.373E+00	0.8045	0.7676
	0.10	0.170E+01	0.8648	0.8394	0.785E+00	0.7996	0.7628	0.499E+00	0.7616	0.7184
	0.20	0.568E+01	0.7559	0.7173	0.241E+01	0.6426	0.5888	0.145E+01	0.5785	0.5174
	0.30	0.157E+02	0.6686	0.6246	0.611E+01	0.5208	0.4623	0.344E+01	0.4400	0.3758
	0.40	0.438E+02	0.5987	0.5539	0.156E+02	0.4271	0.3707	0.820E+01	0.3366	0.2773
	0.50	0.135E+03	0.5429	0.4995	0.443E+02	0.3556	0.3043	0.216E+02	0.2604	0.2093
	0.60	0.508E+03	0.4981	0.4571	0.153E+03	0.3010	0.2557	0.696E+02	0.2048	0.1623
	0.70	0.267E+04	0.4618	0.4235	0.751E+03	0.2594	0.2197	0.317E+03	0.1645	0.1295
	0.80	0.266E+05	0.4322	0.3962	0.699E+04	0.2272	0.1923	0.277E+04	0.1350	0.1061
	0.90	0.128E+07	0.4075	0.3735	0.317E+06	0.2020	0.1709	0.118E+06	0.1132	0.0889
	1.00	INFINITY	0.3865	0.3543	INFINITY	0.1818	0.1538	INFINITY	0.0966	0.0759

$$= \frac{\gamma-1}{\gamma C}\left[1 - (1 - C)^{\gamma/(\gamma-1)}\right] \qquad (\sigma=1) \qquad (9b)$$

$$EI = 1 - \frac{\sigma+1}{\sigma+3}\frac{\gamma}{\gamma-1} C + \frac{\sigma+1}{\sigma+5}\frac{\gamma}{2(\gamma-1)^2} C^2 + 0(C^3) \qquad (10a)$$

$$= \frac{\gamma-1}{(2\gamma-1)C}\left[1 - (1-C)^{(2\gamma-1)/(\gamma-1)}\right] \qquad (\sigma=1) \qquad (10b)$$

Expressions for the case $\sigma = 0,2$ are given in Appendix B. Thus, M_g/M_s and C are further related by

$$\frac{M_g}{M_s} = \frac{2\gamma C}{(\gamma-1)(\sigma+1)}\left[1 + \left(\gamma - \frac{\sigma+1}{\sigma+3}\right)\frac{C}{\gamma-1} + 0(C^2)\right] \qquad (11a)$$

$$= \left(\frac{1}{1-C}\right)^{\gamma/(\gamma-1)} -1 \qquad (\sigma=1) \qquad (11b)$$

The shell trajectory can be expressed in the form

$$\frac{\dot{R}_\infty t}{R_0} = \int_1^{R/R_0} \frac{d(R/R_0)}{\left[1 - (R/R_0)^{-(\gamma-1)(\sigma+1)}\right]^{1/2}} \qquad (12a)$$

$$= \left[(R/R_0)^2-1\right]^{1/2} \qquad (\sigma=2,\ \gamma=5/3) \qquad (12b)$$

$$= \frac{2\left[(R/R_0)- 1\right]^{1/2}}{\left[(\gamma-1)(\sigma+1)\right]^{1/2}}\left[1 + 0\left(\frac{R}{R_0} - 1\right)\right] \qquad (12c)$$

$$= \left(R/R_0\right)\left[1 + 0\,(R_0/R)^{(\gamma-1)(\sigma+1)}\right] \qquad (12d)$$

Corresponding values of $\dot{R}_\infty t/R_0$ and R/R_0 are given in Table 2 for various values of γ and σ. The acceleration of the shell decreases with time, and the shell ultimately moves with the constant velocity $\dot{R}_\infty$ given by Eq. (5c).

Table 2. Shell Ordinate $R = R/R_0$ Versus Time $\text{TAU} = \dot{R}_\infty t/R_0$ for $11/9 \leq \gamma \leq 5/3$ and $\sigma = 0,1,2$

	TAU											
	SIGMA=0.				SIGMA=1.				SIGMA=2.			
	GAMMA	GAMMA	GAMMA	GAMMA	GAMMA	GAMMA	GAMMA	GAMMA	GAMMA	GAMMA	GAMMA	GAMMA
R	5/3	7/5	9/7	11/9	5/3	7/5	9/7	11/9	5/3	7/5	9/7	11/9
1.0	0.0000	0.0000	0.0000	0.0000	0.0000	0.0000	0.0000	0.0000	0.0000	0.0000	0.0000	0.0000
1.5	1.8442	2.3574	2.7774	3.1419	1.3365	1.6919	1.9850	2.2402	1.1180	1.4019	1.6380	1.8443
2.0	2.7494	3.4859	4.0927	4.6206	2.0322	2.5325	2.9508	3.3172	1.7320	2.1235	2.4560	2.7496
2.5	3.5254	4.4390	5.1958	5.8562	2.6487	3.2583	3.7743	4.2291	2.2912	2.7590	3.1645	3.5256
3.0	4.2402	5.3070	6.1954	6.9723	3.2304	3.9304	4.5300	5.0612	2.8284	3.3560	3.8219	4.2405
3.5	4.9184	6.1231	7.1313	8.0149	3.7924	4.5707	5.2448	5.8448	3.3540	3.9310	4.4493	4.9187
4.0	5.5720	6.9038	8.0233	9.0065	4.3419	5.1899	5.9318	6.5954	3.8729	4.4918	5.0568	5.5723
4.5	6.2078	7.6583	8.8828	9.9604	4.8828	5.7938	6.5986	7.3216	4.3874	5.0428	5.6501	6.2081
5.0	6.8299	8.3927	9.7172	10.8849	5.4174	6.3863	7.2500	8.0291	4.8989	5.5865	6.2326	6.8303
5.5	7.4413	9.1109	10.5313	11.7857	5.9474	6.9697	7.8891	8.7217	5.4083	6.1247	6.8068	7.4417
6.0	8.0440	9.8158	11.3287	12.6669	6.4736	7.5459	8.5181	9.4019	5.9160	6.6585	7.3741	8.0444
6.5	8.6394	10.5095	12.1119	13.5316	6.9968	8.1160	9.1388	10.0719	6.4225	7.1888	7.9360	8.6398
7.0	9.2287	11.1937	12.8831	14.3819	7.5177	8.6811	9.7524	10.7331	6.9281	7.7162	8.4932	9.2291
7.5	9.8127	11.8696	13.6437	15.2199	8.0365	9.2419	10.3598	11.3866	7.4330	8.2412	9.0464	9.8132
8.0	10.3921	12.5383	14.3950	16.0469	8.5537	9.7990	10.9619	12.0335	7.9372	8.7641	9.5962	10.3926
8.5	10.9675	13.2006	15.1381	16.8642	9.0694	10.3528	11.5593	12.6745	8.4409	9.2853	10.1430	10.9681
9.0	11.5394	13.8571	15.8739	17.6728	9.5839	10.9037	12.1525	13.3102	8.9442	9.8049	10.6872	11.5399
9.5	12.1081	14.5085	16.6029	18.4735	10.0973	11.4521	12.7420	13.9413	9.4471	10.3232	11.2291	12.1086
10.0	12.6739	15.1552	17.3259	19.2669	10.6097	11.9982	13.3281	14.5680	9.9498	10.8403	11.7689	12.6745

Flow profiles, the net impulse on the plane of symmetry at $r = 0$, and flow conditions at $r_1 \gg r_0$ are now noted.

Flow Profiles: Equation (5) can be expressed

$$\left(\frac{R}{R_0}\right)^{\sigma+1} \frac{\delta R_0^{\sigma+1}}{(\sigma+1)M_g} \rho = \frac{(1 - C\eta^2)^{1/(\gamma-1)}}{MI} \tag{13a}$$

$$\left(\frac{R}{R_0}\right)^{\gamma(\sigma+1)} \frac{\delta R_0^{\sigma+1}}{(\sigma+1)E_g} \frac{p}{\gamma-1} = \frac{(1-C\eta^2)^{\gamma/(\gamma-1)}}{EI} \tag{13b}$$

where ρ and p have been normalized in terms of M_g and E_g, respectively. Equation (13a) is plotted in Fig. 2. Density and pressure are uniform,

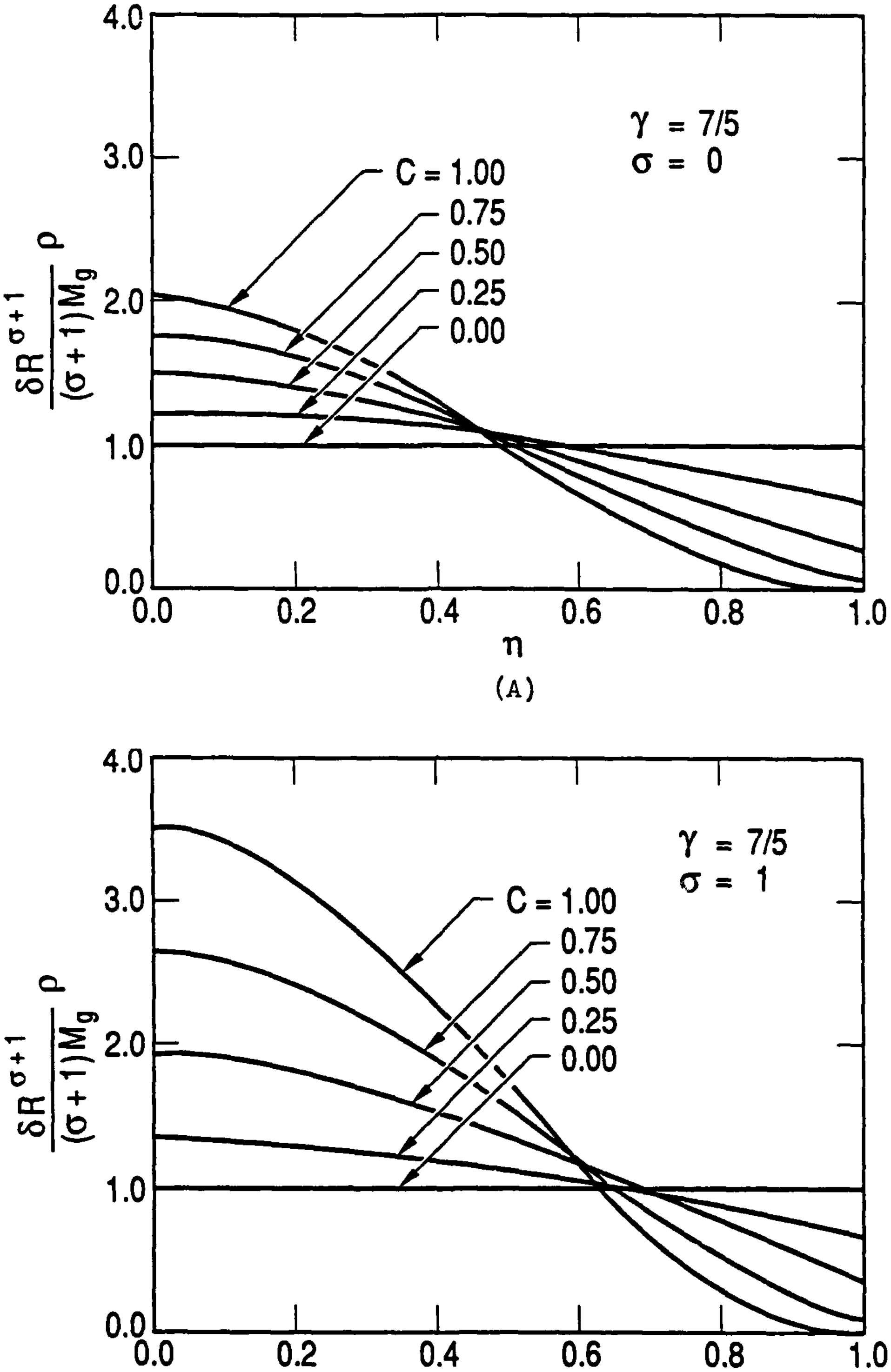

Fig. 2. Gas Density Profile

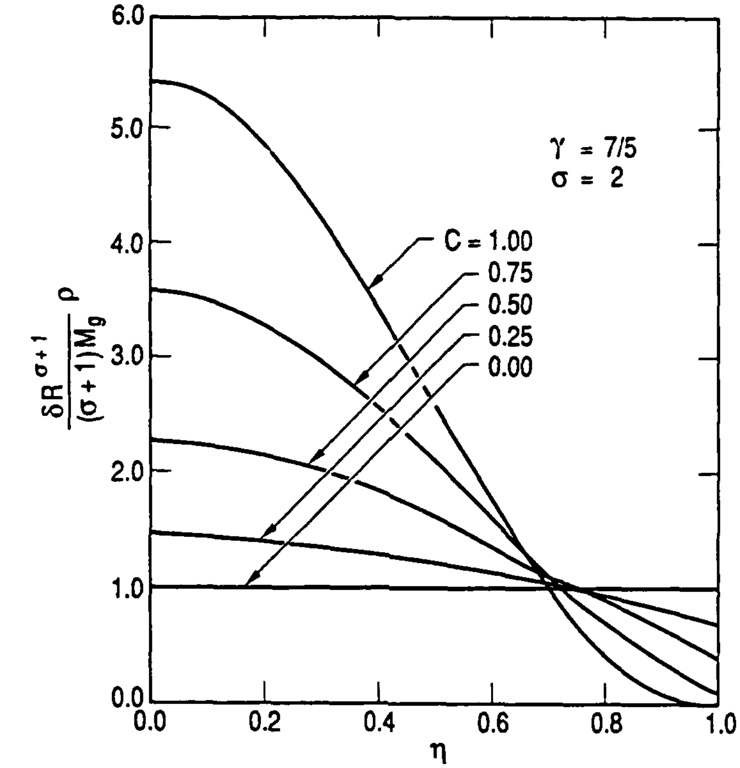

(C)

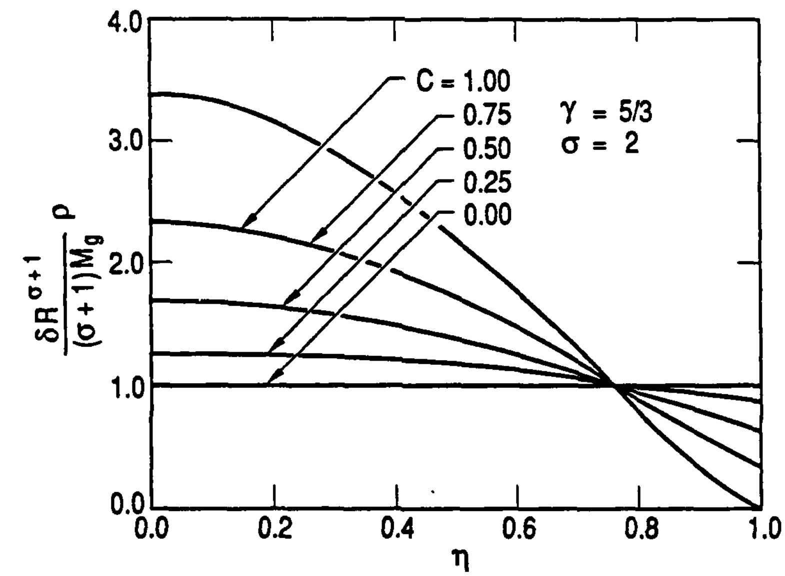

(D)

Fig. 2. Gas Density Profile (Continued)

with η, for the case C = 0. In the latter case the shell mass is large and moves slowly ($\dot{R}_\infty \rightarrow 0$), so that gas density and pressure are equilibrated in the region $0 \leq \eta \leq 1$. The density and pressure decrease at $\eta = 1$, as C increases, and ultimately become zero when C = 1. As previously noted, the case C = 1 corresponds to the expansion into vacuum of an unbound gas.

Impulse at $r = 0$: The net impulse on the plane of symmetry at r = 0 is denoted I_0 and is found from

$$I_0 = \int_0^\infty dt \int_0^A p dA \tag{14}$$

where A = 1,2R, and πR^2 for σ = 0,1, and 2, respectively. The result may be expressed

$$\frac{\dot{R}_\infty I_0}{\delta R_0^{\sigma+1} p_0} = \frac{2B}{(\gamma-1)(\sigma+1)} \tag{15a}$$

where

$$B = 1/2 \qquad \sigma=0 \tag{15b}$$

$$= \frac{1}{\pi} \int_0^1 (1 - C\eta^2)^{\gamma/(\gamma-1)} d\eta = \frac{(EI)_{\sigma=0}}{\pi} \qquad \sigma=1 \tag{15c}$$

$$= \frac{1}{4C} \frac{\gamma-1}{2\gamma-1} \left[1 - (1-C)^{(2\gamma-1)/(\gamma-1)}\right] \qquad \sigma=2 \tag{15d}$$

and $(EI)_{\sigma=0}$ denotes EI evaluated with $\sigma = 0$. Normalization in terms of gas mass and initial gas energy yields

$$\frac{I_0}{(2E_g M_g)^{1/2}} = \left(\frac{(\gamma-1)(\sigma+1)}{2\gamma C \; MI \; EI}\right)^{1/2} B \tag{16a}$$

For $C \rightarrow 0$

$$\left(\frac{M_g}{M_s}\right)^{1/2} \frac{I_0}{(2E_g M_g)^{1/2}} = \frac{1}{2}, \frac{1}{\pi}, \frac{1}{4} \text{ for } \sigma = 0,1,2 \tag{16b}$$

Equation (16a) is listed in Table 3. The net impulse $I_0/(2E_gM_g)^{1/2}$ increases with decrease in C because the shell mass impedes the expansion and thus the pressure at r = 0 remains relatively high for a longer period of time. In the limit $C \to 0$, the initial gas internal energy is transferred to shell kinetic energy.

<u>Flow at $r \gg r_0$</u>: In the limit $r/r_0 \gg 1$, $\dot{R} \to \dot{R}_\infty$ and Eqs. (3) and (5) become

$$v = \dot{R}_\infty \eta \tag{17a}$$

$$R = \dot{R}_\infty t \tag{17b}$$

Let subscript 1 denote conditions at $r_1 \gg r_0$. The variation of gas dynamic pressure with time at this station is

$$\frac{(R_1/R_0)^{\sigma+1}\rho_1 v_1^2}{\rho_0 \dot{R}_\infty^2} = \left(\frac{t_1}{t}\right)^{\sigma+3}\left[1 - C\left(\frac{t_1}{t}\right)^2\right]^{1/(\gamma-1)} \tag{18}$$

where $t_1 = r_1/\dot{R}_\infty$ and $t_1/t \leq 1$. The maximum dynamic pressure is denoted $(\rho_1 v_1^2)_m$ and occurs at time t_m. These can be expressed in the form

$$\frac{\delta R_1^{\sigma+1}(\rho_1 v_1^2)_m}{E_g} = \frac{4\gamma C}{(\gamma-1)EI}\left(\frac{t_1}{t_m}\right)^{\sigma+3}\left[1 - C\left(\frac{t_1}{t_m}\right)^2\right]^{1/(\gamma-1)} \tag{19a}$$

and

$$\frac{t_1}{t_m} = G \qquad G \leq 1 \tag{19b}$$

$$= 1 \qquad G > 1 \tag{19c}$$

Table 3. Net Impulse at Plane of Symmetry IM $\equiv I_0/(2M_gE_g)^{1/2}$ for $11/9 \leq \gamma \leq 5/3$, $\sigma = 0,1,2$ and $0.02 \leq C \leq 1.00$.

		IM		
GAMMA	C	SIGMA=0.0	SIGMA=1.0	SIGMA=2
1.667	0.00	∞	∞	∞
	0.02	1.602	1.428	1.368
	0.04	1.148	1.014	0.967
	0.06	0.950	0.831	0.789
	0.08	0.834	0.722	0.683
	0.10	0.756	0.649	0.610
	0.20	0.571	0.469	0.431
	0.30	0.499	0.394	0.353
	0.40	0.461	0.352	0.309
	0.50	0.440	0.326	0.280
	0.60	0.428	0.310	0.261
	0.70	0.421	0.301	0.249
	0.80	0.417	0.295	0.242
	0.90	0.416	0.293	0.238
	1.00	0.416	0.292	0.238
1.400	0.00	∞	∞	∞
	0.02	1.363	1.211	1.159
	0.04	0.983	0.863	0.820
	0.06	0.819	0.709	0.671
	0.08	0.723	0.619	0.582
	0.10	0.660	0.558	0.522
	0.20	0.513	0.412	0.374
	0.30	0.459	0.353	0.312
	0.40	0.434	0.323	0.278
	0.50	0.422	0.306	0.258
	0.60	0.416	0.297	0.246
	0.70	0.413	0.292	0.240
	0.80	0.412	0.291	0.237
	0.90	0.412	0.290	0.236
	1.00	0.412	0.290	0.236
1.286	0.00	∞	∞	∞
	0.02	1.210	1.072	1.024
	0.04	0.879	0.766	0.726
	0.06	0.736	0.632	0.595
	0.08	0.654	0.554	0.518
	0.10	0.600	0.501	0.465
	0.20	0.479	0.377	0.338
	0.30	0.438	0.330	0.287
	0.40	0.421	0.307	0.261
	0.50	0.414	0.296	0.247
	0.60	0.410	0.291	0.240
	0.70	0.409	0.289	0.236
	0.80	0.409	0.289	0.235
	0.90	0.409	0.289	0.235
	1.00	0.409	0.289	0.235
1.222	0.00	∞	∞	∞
	0.02	1.102	0.973	0.928
	0.04	0.805	0.698	0.660
	0.06	0.679	0.578	0.542
	0.08	0.606	0.508	0.473
	0.10	0.559	0.461	0.426
	0.20	0.458	0.354	0.314
	0.30	0.426	0.315	0.271
	0.40	0.414	0.299	0.250
	0.50	0.409	0.291	0.241
	0.60	0.408	0.289	0.236
	0.70	0.407	0.288	0.235
	0.80	0.407	0.288	0.235
	0.90	0.407	0.288	0.234
	1.00	0.407	0.288	0.234

where

$$G = \frac{1}{C^{1/2}} \left[\frac{(\sigma+3)(\gamma-1)}{(\sigma+3)(\gamma-1) + 2}\right]^{1/2} \tag{19d}$$

In the limit $C \to 0$,

$$t_1/t_m = 1 \tag{20a}$$

$$\frac{\delta R_1^{\sigma+1} \, (\rho_1 v_1^{\,2})_m}{E_g} = 2(\sigma+1) \frac{M_g}{M_s} [1 + O(C)] \tag{20b}$$

Numerical results for $(\rho_1 v_1^{\,2})_m$ and t_m are given in Table 4. Values of t_1/t_m in the range $t_1/t_m < 1$ indicate a local maximum in dynamic pressure. The case $t_1/t_m = 1$ corresponds to a flow wherein the maximum dynamic pressure occurs directly behind the shell. The maximum dynamic pressure is seen to decrease with decrease in C (i.e., increase in shell mass). The latter trend occurs because, at a fixed location r_1, the gas density is relatively unaffected by the shell whereas the flow velocities are decreased due to shell inertia.

The impulse per unit area at r_1, due to gas flux, is denoted I_g and is found from

$$\frac{(R_1/R_0)^{\sigma+1} I_g}{\rho_0 \, \dot{R}_\infty^{\,2} \, t_1} = \frac{(R_1/R_0)^{\sigma+1}}{\rho_0 \dot{R}_\infty^{\,2} \, t_1} \int_{t_1}^{\infty} \rho_1 v_1^{\,2} \, dt$$

$$= \int_0^1 \left(\frac{t_1}{t}\right)^{\sigma+1} \left[1 - C\left(\frac{t_1}{t}\right)^2\right]^{1/(\gamma-1)} d(t_1/t)$$

Table 4. Maximum Dynamic Pressure MDP $\equiv \delta R_1^{\sigma+1}(\rho_1 v_1^2)_m/E_g$
Corresponding Time XM $\equiv t_1/t_m$ for $r_1 >> r_0$,
$11/9 \le \gamma \le 5/3$, $\sigma = 0,1,2$ and $0.02 \le C \le 1.00$

		SIGMA=0.0		SIGMA=1.0		SIGMA=2.0	
GAMMA	C	XM	MDP	XM	MDP	XM	MDP
1.667	0.00	1.0000	0.0000	1.0000	0.0000	1.0000	0.0000
	0.02	1.0000	0.1973	1.0000	0.1989	1.0000	0.2000
	0.04	1.0000	0.3890	1.0000	0.3956	1.0000	0.3997
	0.06	1.0000	0.5748	1.0000	0.5897	1.0000	0.5990
	0.08	1.0000	0.7544	1.0000	0.7809	1.0000	0.7976
	0.10	1.0000	0.9277	1.0000	0.9689	1.0000	0.9952
	0.20	1.0000	1.6876	1.0000	1.8480	1.0000	1.9569
	0.30	1.0000	2.2453	1.0000	2.5873	1.0000	2.8365
	0.40	1.0000	2.5688	1.0000	3.1256	1.0000	3.5641
	0.50	1.0000	2.6338	1.0000	3.3936	1.0000	4.0443
	0.60	0.9129	2.5833	0.9759	3.3418	1.0000	4.1572
	0.70	0.8452	2.5591	0.9035	3.2546	0.9449	3.9723
	0.80	0.7906	2.5494	0.8452	3.2180	0.8839	3.8823
	0.90	0.7454	2.5468	0.7968	3.2075	0.8333	3.8553
	1.00	0.7071	2.5465	0.7559	3.2065	0.7906	3.8526
1.400	0.00	1.0000	0.0000	1.0000	0.0000	1.0000	0.0000
	0.02	1.0000	0.2725	1.0000	0.2757	1.0000	0.2777
	0.04	1.0000	0.5297	1.0000	0.5424	1.0000	0.5503
	0.06	1.0000	0.7712	1.0000	0.7995	1.0000	0.8172
	0.08	1.0000	0.9969	1.0000	1.0463	1.0000	1.0778
	0.10	1.0000	1.2064	1.0000	1.2822	1.0000	1.3314
	0.20	1.0000	2.0055	1.0000	2.2766	1.0000	2.4686
	0.30	1.0000	2.3896	1.0000	2.9088	1.0000	3.3133
	0.40	0.9682	2.3998	1.0000	3.1245	1.0000	3.7600
	0.50	0.8660	2.3466	0.9428	2.9952	1.0000	3.7217
	0.60	0.7906	2.3234	0.8607	2.9099	0.9129	3.5160
	0.70	0.7319	2.3146	0.7968	2.8756	0.8452	3.4295
	0.80	0.6847	2.3120	0.7454	2.8649	0.7906	3.4011
	0.90	0.6455	2.3115	0.7027	2.8629	0.7454	3.3956
	1.00	0.6124	2.3115	0.6667	2.8628	0.7071	3.3953
1.286	0.00	1.0000	0.0000	1.0000	0.0000	1.0000	0.0000
	0.02	1.0000	0.3456	1.0000	0.3509	1.0000	0.3541
	0.04	1.0000	0.6623	1.0000	0.6828	1.0000	0.6956
	0.06	1.0000	0.9500	1.0000	0.9950	1.0000	1.0236
	0.08	1.0000	1.2090	1.0000	1.2866	1.0000	1.3369
	0.10	1.0000	1.4395	1.0000	1.5568	1.0000	1.6345
	0.20	1.0000	2.1809	1.0000	2.5654	1.0000	2.8496
	0.30	1.0000	2.3178	1.0000	2.9753	1.0000	3.5221
	0.40	0.8660	2.2413	0.9534	2.8636	1.0000	3.5790
	0.50	0.7746	2.2109	0.8528	2.7519	0.9129	3.3214
	0.60	0.7071	2.1998	0.7785	2.7087	0.8333	3.2121
	0.70	0.6546	2.1965	0.7207	2.6947	0.7715	3.1747
	0.80	0.6124	2.1958	0.6742	2.6915	0.7217	3.1655
	0.90	0.5773	2.1957	0.6356	2.6911	0.6804	3.1644
	1.00	0.5477	2.1957	0.6030	2.6911	0.6455	3.1644
1.222	0.00	1.0000	0.0000	1.0000	0.0000	1.0000	0.0000
	0.02	1.0000	0.4167	1.0000	0.4245	1.0000	0.4292
	0.04	1.0000	0.7871	1.0000	0.8170	1.0000	0.8359
	0.06	1.0000	1.1122	1.0000	1.1769	1.0000	1.2185
	0.08	1.0000	1.3931	1.0000	1.5031	1.0000	1.5757
	0.10	1.0000	1.6313	1.0000	1.7952	1.0000	1.9061
	0.20	1.0000	2.2471	1.0000	2.7375	1.0000	3.1157
	0.30	0.9128	2.2026	1.0000	2.8675	1.0000	3.5277
	0.40	0.7905	2.1511	0.8770	2.6847	0.9449	3.2726
	0.50	0.7071	2.1333	0.7844	2.6166	0.8451	3.1025
	0.60	0.6455	2.1280	0.7161	2.5944	0.7715	3.0435
	0.70	0.5976	2.1267	0.6630	2.5887	0.7143	3.0274
	0.80	0.5590	2.1265	0.6202	2.5877	0.6681	3.0244
	0.90	0.5270	2.1265	0.5847	2.5877	0.6299	3.0242
	1.00	0.5000	2.1265	0.5547	2.5877	0.5976	3.0242

Integration yields

$$\frac{(R_1/R_0)^{\sigma+1} I_g}{\rho_0 \dot{R}_\infty^2 t_1} = \frac{\gamma-1}{2\gamma C} \left[1 - (1-C)^{\gamma/(\gamma-1)}\right] \qquad \sigma=0 \qquad (21a)$$

$$= \frac{1}{3} (MI)_{\sigma=2} \qquad \sigma=1 \qquad (21b)$$

$$= \frac{\gamma-1}{2\gamma C} \left\{\frac{\gamma-1}{(2\gamma-1)C} \left[1 - (1-C)^{(2\gamma-1)/(\gamma-1)}\right] - (1-C)^{\gamma/(\gamma-1)}\right\} \qquad \sigma=2 \qquad (21c)$$

where $(MI)_{\sigma=2}$ indicates that MI is evaluated with $\sigma = 2$. The impulse per unit area at r_1 due to the shell is $I_s \equiv M_s \dot{R}_\infty/(\delta R_1^\sigma)$, which can be expressed

$$\frac{(R_1/R_0)^{\sigma+1} I_s}{\rho_0 \dot{R}_\infty^2 t_1} = \frac{\gamma-1}{2\gamma C} [1-C]^{\gamma/(\gamma-1)} \qquad (22)$$

The expressions for I_g and I_s can be put in the form

$$\frac{\delta R_1^\sigma I_g}{(2M_g E_g)^{1/2}} = \left(\frac{2\gamma C(\sigma+1)}{(\gamma-1)MI\ EI}\right)^{1/2} \frac{(R_1/R_0)^{\sigma+1} I_g}{\rho_0 \dot{R}_\infty^2 t_1} \qquad (23a)$$

$$\frac{\delta R_1^\sigma I_s}{(2M_g E_g)^{1/2}} = \left(\frac{(\sigma+1)(\gamma-1)}{2\gamma C\ MI\ EI}\right)^{1/2} (1-C)^{\gamma/(\gamma-1)} \qquad (23b)$$

wherein $\delta R_1^{\sigma} I_g$ and $\delta R_1^{\sigma} I_s$ are referenced to the net impulse associated with a free gas expansion. In the limit $C \rightarrow 0$, Eqs. (23a) and (23b) become

$$\left(\frac{M_g}{M_s}\right)^{1/2} \frac{\delta R_1^{\sigma} I_g}{(2M_g E_g)^{1/2}} = \frac{\sigma+1}{\sigma+2} \frac{M_g}{M_s} \tag{24a}$$

$$\left(\frac{M_g}{M_s}\right)^{1/2} \frac{\delta R_1^{\sigma} I_s}{(2M_g E_g)^{1/2}} = 1 \tag{24b}$$

In the limit $C \rightarrow 0$, the shell kinetic energy $M_s \dot{R}_{\infty}^2/2$ equals the original gas internal energy E_g and the quantity $\delta R_1^{\sigma} I_s$ corresponds to the net momentum of a mass M_s with kinetic energy E_g.

Numerical results for I_g, I_s and $I_t = I_g + I_s$ are given in Table 5. The quantities $\delta R_1^{\sigma} I_t/(2M_g E_g)^{1/2}$ and $\delta R_1^{\sigma} I_s/(2M_g E_g)^{1/2}$ increase while $\delta R_1^{\sigma} I_g/ (2M_g E_g)^{1/2}$ decreases as C decreases. This behavior is again due to the reduction in gas expansion rate as C decreases.

B. APPROXIMATE LOCAL SIMILARITY SOLUTION

The problem is now generalized to include a highly compressible porous medium external to the shell. The configuration is illustrated in Fig. 3. As the shell expands, the porous medium is compressed and adheres to the shell in the form of a thin band (i.e., an inelastic collision is assumed). The subsequent motion is deduced herein using a local similarity approximation.

Let $M_{s,0}$ denote the mass of the shell at $t = 0$, let M_s denote the mass of the shell at subsequent times, and let ρ_p denote the density of the porous medium. The shell mass at any instant can be expressed

$$\frac{M_s}{M_g} = \frac{M_{s,0}}{M_g} + \alpha(Y-1) \tag{25a}$$

Table 5. Impulse per Unit Area at $r_1 \gg r_0$ Due to Gas $IMG \equiv \delta R_1^{\sigma} I_g/(2M_gE_g)^{1/2}$, Due to Shell $IMS \equiv \delta R_1^{\sigma} I_s/(2M_gE_g)^{1/2}$ and Due to Sum $IMT \equiv IMG + IMS$ as a Function of $11/9 \le \gamma \le 5/3$, $\sigma = 0,1,2$ and $0.02 \le C \le 1.00$.

		SIGMA=0.0			SIGMA=1.0			SIGMA=2.0		
GAMMA	C	IMG	IMS	IMT	IMG	IMS	IMT	IMG	IMS	IMT
1.667	0.00	0.0000	∞	∞	0.0000	∞	∞	0.0000	∞	∞
	0.02	0.1578	3.0469	3.2048	0.1494	4.3381	4.4875	0.1375	5.3346	5.4721
	0.04	0.2228	2.0738	2.2966	0.2116	2.9728	3.1844	0.1952	3.6709	3.8661
	0.06	0.2723	1.6280	1.9003	0.2597	2.3501	2.6097	0.2400	2.9144	3.1544
	0.08	0.3138	1.3540	1.6679	0.3003	1.9685	2.2689	0.2782	2.4519	2.7301
	0.10	0.3501	1.1618	1.5118	0.3364	1.7012	2.0375	0.3123	2.1284	2.4407
	0.20	0.4886	0.6542	1.1428	0.4788	0.9949	1.4737	0.4498	1.2753	1.7251
	0.30	0.5883	0.4088	0.9971	0.5885	0.6477	1.2362	0.5602	0.8534	1.4136
	0.40	0.6649	0.2571	0.9221	0.6792	0.4258	1.1050	0.6559	0.5789	1.2348
	0.50	0.7242	0.1555	0.8797	0.7550	0.2700	1.0250	0.7403	0.3803	1.1206
	0.60	0.7688	0.0866	0.8553	0.8169	0.1579	0.9748	0.8136	0.2315	1.0451
	0.70	0.8002	0.0415	0.8417	0.8645	0.0797	0.9442	0.8741	0.1221	0.9962
	0.80	0.8200	0.0149	0.8349	0.8970	0.0303	0.9273	0.9186	0.0486	0.9672
	0.90	0.8295	0.0026	0.8322	0.9142	0.0056	0.9199	0.9440	0.0095	0.9535
	1.00	0.8317	0.0000	0.8317	0.9183	0.0000	0.9183	0.9505	0.0000	0.9505
1.400	0.00	0.0000	∞	∞	0.0000	∞	∞	0.0000	∞	∞
	0.02	0.1861	2.5403	2.7265	0.1764	3.6290	3.8054	0.1624	4.4718	4.6342
	0.04	0.2618	1.7048	1.9666	0.2494	2.4605	2.7098	0.2303	3.0509	3.2812
	0.06	0.3189	1.3188	1.6377	0.3053	1.9235	2.2288	0.2827	2.4004	2.6832
	0.08	0.3661	1.0804	1.4465	0.3523	1.5925	1.9448	0.3272	2.0006	2.3278
	0.10	0.4069	0.9124	1.3193	0.3936	1.3595	1.7531	0.3666	1.7196	2.0862
	0.20	0.5565	0.4701	1.0266	0.5524	0.7413	1.2937	0.5228	0.9729	1.4957
	0.30	0.6553	0.2637	0.9190	0.6674	0.4417	1.1091	0.6425	0.6046	1.2470
	0.40	0.7233	0.1453	0.8686	0.7546	0.2594	1.0140	0.7394	0.3721	1.1115
	0.50	0.7689	0.0746	0.8435	0.8195	0.1420	0.9615	0.8170	0.2147	1.0317
	0.60	0.7976	0.0336	0.8312	0.8645	0.0685	0.9330	0.8755	0.1094	0.9849
	0.70	0.8135	0.0122	0.8257	0.8923	0.0265	0.9188	0.9148	0.0449	0.9597
	0.80	0.8208	0.0029	0.8237	0.9061	0.0068	0.9129	0.9361	0.0122	0.9484
	0.90	0.8229	0.0003	0.8232	0.9107	0.0006	0.9113	0.9437	0.0012	0.9449
	1.00	0.8231	0.0000	0.8231	0.9111	0.0000	0.9111	0.9446	0.0000	0.9446
1.286	0.00	0.0000	∞	∞	0.0000	∞	∞	0.0000	∞	∞
	0.02	0.2103	2.2100	2.4204	0.1996	3.1678	3.3674	0.1839	3.9114	4.0953
	0.04	0.2949	1.4621	1.7570	0.2816	2.1247	2.4063	0.2604	2.6455	2.9059
	0.06	0.3578	1.1146	1.4724	0.3439	1.6423	1.9862	0.3192	2.0626	2.3818
	0.08	0.4093	0.8990	1.3083	0.3959	1.3436	1.7395	0.3688	1.7025	2.0713
	0.10	0.4532	0.7471	1.2003	0.4412	1.1327	1.5739	0.4125	1.4486	1.8610
	0.20	0.6076	0.3513	0.9589	0.6105	0.5741	1.1846	0.5820	0.7717	1.3536
	0.30	0.7007	0.1761	0.8768	0.7250	0.3114	1.0363	0.7053	0.4428	1.1481
	0.40	0.7576	0.0845	0.8421	0.8040	0.1619	0.9659	0.7979	0.2451	1.0430
	0.50	0.7905	0.0365	0.8271	0.8555	0.0758	0.9313	0.8641	0.1226	0.9867
	0.60	0.8076	0.0133	0.8209	0.8855	0.0297	0.9153	0.9067	0.0515	0.9582
	0.70	0.8151	0.0036	0.8187	0.9001	0.0087	0.9089	0.9295	0.0162	0.9457
	0.80	0.8176	0.0006	0.8181	0.9054	0.0015	0.9069	0.9386	0.0030	0.9415
	0.90	0.8180	0.0000	0.8181	0.9065	0.0001	0.9066	0.9406	0.0001	0.9407
	1.00	0.8180	0.0000	0.8180	0.9066	0.0000	0.9066	0.9407	0.0000	0.9407

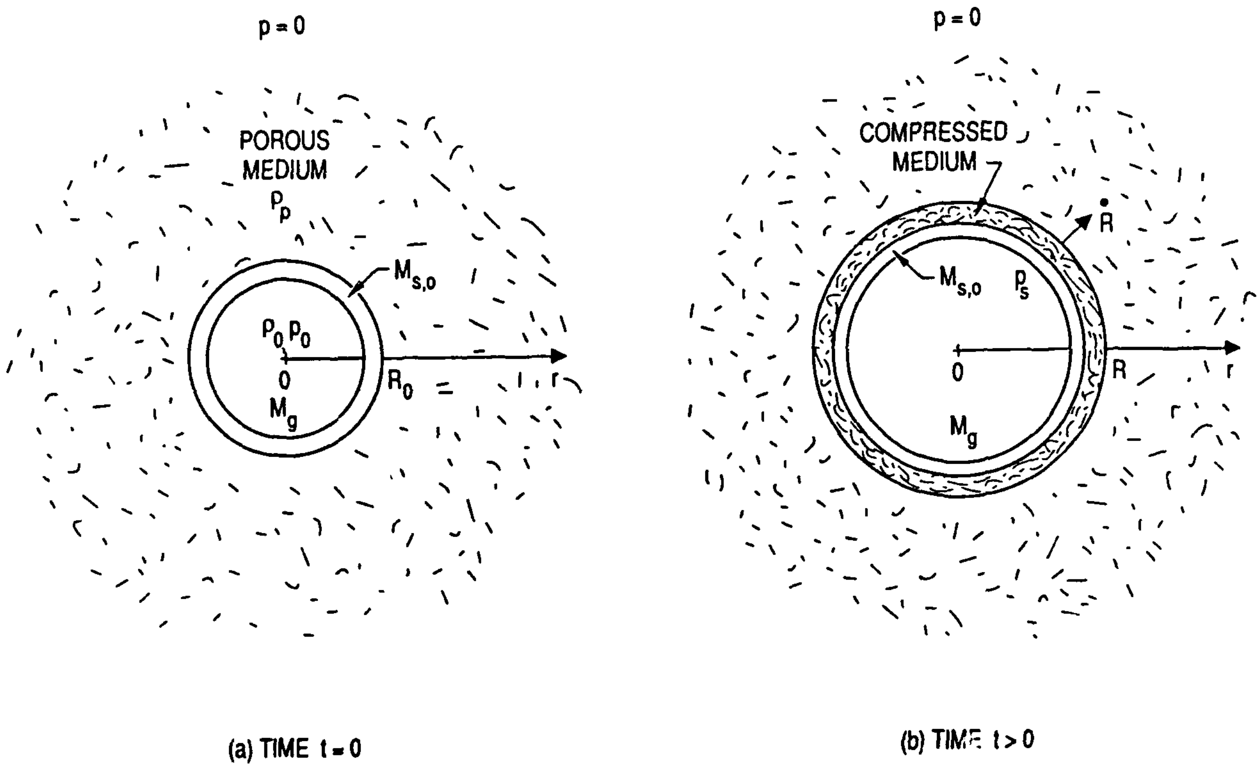

Fig. 3. Expansion of Gas Bound by Shell and Porous Medium

where

$$\alpha = \frac{\rho_p \; \delta \; R_0^{\sigma+1}}{(\sigma+1) \; M_g} = \frac{1}{(MI)_0} \; \frac{\rho_p}{\rho_0} \tag{25b}$$

$$Y = (R/R_0)^{\sigma+1} \tag{25c}$$

and $(MI)_0$ denotes the value of MI at $t = 0$. Conservation of momentum can be expressed in the form

$$\delta R^\sigma \; p_s = d(M_s \dot{R})/dt \tag{26}$$

Integration yields

$$\frac{(M_s \dot{R})^2}{2 M_g E_g} = \frac{\gamma - 1}{(EI)_0} \int_1^Y \frac{M_s}{M_g} \frac{p_s}{p_0} \, dY \tag{27}$$

where E_g again denotes net internal gas energy at $t = 0$ and where $(EI)_0$ denotes the value of EI at $t = 0$. In order to integrate Eq. (27), it is necessary to express p_s/p_0 as a function of M_s/M_g or Y. The assumption of local similarity is now introduced. Namely, it is assumed that at each instant the local fluid property values equal those for a self-similar flow with the same values of M_s/M_g and Y. Thus, recalling Eqs. (5a) and (8a), flow properties are given by

$$\frac{\rho}{\rho_0} = \left(\frac{p}{p_0}\right)^{1/\gamma} = \frac{1 - C\eta^2}{Y} \; \frac{(MI)_0}{MI}$$

$$v/R = \eta$$

and p_s/p_0 can be expressed in the form

$$\frac{p_s}{p_0} = \frac{\phi Y^{-\gamma}}{1 + [(\sigma+1)/2](M_g/M_s)} \tag{28a}$$

where

$$\phi = \frac{\gamma C\,MI}{\gamma-1}\left[1+\frac{2}{\sigma+1}\frac{M_s}{M_g}\right]\left[\frac{(MI)_0}{MI}\right]^{\gamma}$$
$$\equiv \psi\left[(MI)_0/MI\right]^{\gamma} \qquad (28b)$$

For $\sigma = 1$

$$\psi = 1$$

$$MI = \frac{\gamma-1}{\gamma}\,\frac{M_g/M_s}{1+(M_g/M_s)-\left[1+(M_g/M_s)\right]^{1/\gamma}}$$

The dependence of ψ on M_s/M_g, for $\sigma = 0$ and 2, has the limiting values

$$\psi = 1 \qquad M_g/M_s = 0 \ (C = 0)$$

$$= \frac{\gamma\,MI}{\gamma-1} \qquad M_s/M_g = 0 \ (C = 1)$$

It is seen that ϕ is an order 1 quantity and has a weak dependence on M_s/M_g. Thus, the major dependence of p_s/p_0 on M_g/M_s is explicitly displayed in Eq. (28a). Substitution into Eq. (27) yields

$$\frac{(M_s\dot{R})^2}{2M_gE_g} = \frac{\gamma-1}{(EI)_0}\int_1^Y \frac{(M_s/M_g)^2}{B+\alpha Y}\,\phi Y^{-\gamma}\,dY \qquad (29)$$

where

$$B = \frac{\sigma+1}{2} + \frac{M_{s,0}}{M_g} - \alpha$$

Equation (29) can be integrated to obtain $M_s\dot{R}$ as a function of Y. The dependence of ϕ on M_s/M_g is found from Eq. (28b). The shell trajectory is found from

$$\left(\frac{2E_g}{M_g}\right)^{1/2} \frac{t}{R_0} = \int_1^{R/R_0} \frac{M_s}{M_g} \frac{(2M_gE_g)^{1/2}}{M_s\dot{R}} \frac{dR}{R_0} \tag{30}$$

Limiting cases are now noted. In the limits $\alpha Y \ll B$, $\alpha Y \gg B$, and $B = 0$, Eq. (29) becomes, respectively,

$$\frac{(EI)_0}{\gamma-1} \frac{(M_s\dot{R})^2}{2M_gE_g} = \frac{1}{B} \int_1^Y \phi\, Y^{-\gamma} \left(\frac{M_s}{M_g}\right)^2 \left[1 - \frac{\alpha Y}{B} + O\left(\frac{\alpha Y}{B}\right)^2\right] dY \tag{31a}$$

$$= \frac{1}{\alpha} \int_1^Y \phi\, Y^{-\gamma-1} \left(\frac{M_s}{M_g}\right)^2 \left[1 - \frac{B}{\alpha Y} + O\left(\frac{B}{\alpha Y}\right)^2\right] dY \tag{31b}$$

$$= \frac{1}{\alpha} \int_1^Y \phi\, Y^{-\gamma-1} \left(\frac{M_s}{M_g}\right)^2 dY \qquad (B = 0) \tag{31c}$$

These can be readily integrated analytically if a mean value of ϕ is used. Equation (31a) treats the case where the porous medium introduces only small departures from a self-similar flow. Equation (31b) treats a porous medium at late times. Equation (31c) provides a particular case which is valid for all values of αY.

In the limit $\alpha Y \to 0$, $M_s \to M_{s,0}$, the flow is self-similar. Equation (31a) yields

$$\frac{(M_{s,0}\dot{R})^2}{2M_gE_g} = \frac{\phi}{(EI)_0} \frac{(M_{s,0}/M_g)^2}{M_{s,0}/M_g + (\sigma+1)/2} (1-Y^{1-\gamma}) \tag{32}$$

which agrees with Eq. (5b). The role of $M_{s,0}/M_g$ is explicitly displayed in Eq. (32) except for the weak dependence of ϕ on $M_{s,0}/M_g$.

The limit $\alpha Y \to \infty$ corresponds to the case of a porous medium and large distances from the origin. In this limit the shell trajectory, velocity, momentum, and kinetic energy are, respectively,

$$\frac{R}{R_0} = \left\{\frac{[\gamma(\sigma+1) + 2]^2}{4} \frac{\gamma-1}{2-\gamma} \frac{(MI)_0^\gamma}{(EI)_0} \frac{2E_g t^2}{\alpha M_g R_0^2}\right\}^{1/[\gamma(\sigma+1)+2]} \tag{33a}$$

$$\left(\frac{M_g}{2E_g}\right)^{1/2} \dot{R} = \left[\frac{\gamma-1}{2-\gamma} \frac{(MI)_0^\gamma}{(EI)_0} \frac{1}{\alpha Y^\gamma}\right]^{1/2} \tag{33b}$$

$$\frac{M_s \dot{R}}{(2M_g E_g)^{1/2}} = \left[\frac{\gamma-1}{2-\gamma} \frac{(MI)_0^\gamma}{(EI)_0} \alpha Y^{2-\gamma}\right]^{1/2} \tag{33c}$$

$$\frac{M_s \dot{R}^2}{2E_g} = \frac{\gamma-1}{2-\gamma} \frac{(MI)_0{}^\gamma}{(EI)_0} \frac{1}{Y^{\gamma-1}} \tag{33d}$$

It is seen that shell radius and shell momentum increase with Y, whereas shell velocity and shell kinetic energy decrease with Y. The decrease in kinetic energy is due to the assumption of inelastic collisions between the shell and the porous medium.

It is also seen from Eqs. (32) and (33b) that when the expanding gas is bound by a shell and a porous medium, the shell velocity increases to some maximum value and then decreases during the expansion process. This behavior can be illustrated by considering the limit $M_g/M_{s,0} \ll 1$, $\alpha = O(1)$. In this limit $(EI)_0 = \phi = 1$, $B = M_{s,0}/M_g$ and $M_s/M_g = (M_{s,0}/M_g) + \alpha Y$. Equation (29) becomes

$$\frac{(M_s \dot{R})^2}{2M_g E_g} = \frac{M_{s,0}}{M_g} \left[1 - \frac{1}{Y^{\gamma-1}}\right] + \frac{(\gamma-1)\alpha}{2-\gamma} \left[Y^{2-\gamma} - 1\right] \tag{34}$$

The first term in the right-hand side of Eq. (34) corresponds to a shell without a porous medium and agrees with Eq. (32) in the limit $M_g/M_{s,0} \to 0$. The second term in the right-hand side of Eq. (34) indicates the effect of

a porous medium and, in the limit $\alpha Y \to \infty$, agrees with Eq. (33b). Equation (34) provides a solution which is valid for all values of Y.

A solution for a strong explosion in an infinite porous medium is presented in Ref. 2. That solution assumes that the decrease in kinetic energy of the mass M_s in time dt is equal to the increase in the kinetic energy of the mass dM_s encompassed by the shell in the time dt. For the case of an extremely porous medium, this relation becomes

$$- \frac{d}{dt} \left(\frac{M_s \dot{R}^2}{2}\right) = \frac{\dot{R}^2}{2} \frac{dM_s}{dt}$$

which can be put in the form

$$\frac{d(M_s \dot{R})}{dt} = 0 \tag{35}$$

Integration indicates

$$M_s \dot{R} = \text{CONST} \tag{36a}$$

$$\frac{M_s \dot{R}^2}{2} = \frac{(\text{CONST})^2}{2M_s} \sim \frac{1}{Y} \tag{36b}$$

The constant of integration is undefined in Ref. 2. Equations (36a) and (36b) indicate conservation of shell momentum and a decrease in shell kinetic energy with increase in Y. The present analysis, Eq. (33), indicates an increase in momentum and a slower decrease of kinetic energy with increase in Y. The difference is due to the fact that the present analysis includes the effect of gas pressure on shell momentum [Eq. (26)], while Ref. 2 does not, [Eq. (35)]. This difference is a consequence of the present assumption that the shell bounds the gas during the entire expansion.

III. CONCLUDING REMARKS

The expansion into vacuum of a gas bound by a shell-like mass with zero tension has been evaluated. The flow is self-similar.[1] The effect of the shell is to reduce expansion velocities, reduce gas dynamic pressure, and increase the net impulse at a station.

An approximate local similarity solution has been presented for the case where the shell is surrounded by a highly compressible porous medium. The shell mass at each instant during the expansion is assumed to equal the original shell mass plus the mass of the displayed porous medium. In the limit $R/R_0 \gg 1$, the net shell momentum increases with increase in R/R_0. The latter result differs from the corresponding solution for a point explosion in a porous medium in Ref. 2 due to inclusion herein of the effect of gas pressure on late time shell motion.

REFERENCES

1. L. I. Sedov, Similarity and Dimensional Methods in Mechanics, (Academic Press, New York, 1959), pp 271-281.

2. Y. B. Zeldovich, and Y. P. Raizer, Physics of Shock Waves and High Temperature Hydrodynamic Phenomena, (Academic Press, New York, 1967), pp. 847-849.

APPENDIX A
SYMBOLS

a_0	speed of sound at $(r,t) = (0, 0)$
C	constant related to M_g/M_s, Eq. (8c)
E_g	initial energy of gas
EI	normalized energy integral, Eq. (8b)
I_0	net impulse at plane of symmetry at $r = 0$, Eq. (14)
I_g	impulse per unit area at $r_1 >> r_0$ due to gas flow, Eq. (21)
I_s	impulse per unit area at $r_1 >> r_0$ due to shell, Eq. (22)
I_t	$I_g + I_s$
M_g	mass of gas
M_s	mass of shell
MI	normalized mass integral, Eq. (8a)
p	gas pressure
p_s	gas pressure at $\eta = 1$
p_0	gas pressure at $(r,t) = (0,0)$
R	shell location, $R(t)$
R_0	initial shell location
r	radial distance
r_0	intial edge of gas cloud, $r_0 = R_0$
r_1	radial distance satisfying $r_1 >> r_0$
t	time
v	velocity in r direction
γ	ratio specific heats
δ	2, 2π and 4π for $\sigma = 0,1$ and 2
η	similarity variable, r/R
ρ	gas density
ρ_0	gas density at $(r,t) = (0,0)$
ρ_p	density of porous medium
σ	0,1 and 2 for planar, cylindrical and spherical flows

Subscript

0 conditions at $(r,t) = (0,0)$ or at $t = 0$

1 condition at $r_1 \gg r_0$

Superscript

$(\dot{\ })$ $d(\ )/dt$

APPENDIX B
INTEGRALS FOR MI AND EI

Integral expressions for MI and EI are given by Eqs. (8a) and (8b). These have been integrated in closed form. The results for $\sigma = 1$ are given in Eqs. (9b) and (10b). The results for $\sigma = 0,2$ are given herein.

The integral expression for MI and EI can be put in the form

$$MI;\ EI = (\sigma+1) \int_0^1 (1-C\eta^2)^{(N-1)/2} \eta^\sigma d\eta \qquad \text{(B-1a)}$$

where, for MI

$$N = (\gamma+1)/(\gamma-1) \qquad \text{(B-1b)}$$

and for EI

$$N = (3\gamma-1)/(\gamma-1) \qquad \text{(B-1c)}$$

For γ = 5/3, 7/5, 9/7,... the parameter N has the values 4,6,8,... and 6,8,10,... for MI and EI, respectively. The substitution $C^{1/2}\eta = \sin\theta$ yields

$$MI;\ EI = \frac{\sigma+1}{C^{(\sigma+1)/2}} \int_0^{\sin^{-1}C^{1/2}} (\cos^N\theta - \frac{\sigma}{2}\cos^{N+2})d\theta \qquad \text{(B-2)}$$

Since N is an even integer for cases of interest, Eq. (B-2) can be integrated to yield (for $\sigma = 0,2$)

$$\mathrm{MI;\ EI} = \frac{\sigma+1}{C^{\sigma/2}}\left(1 - \frac{\sigma}{2}\,\frac{N+1}{N+2}\right)\left[\frac{(1-C)^{(N-1)/2}}{N} + \frac{N-1}{N}\,\frac{(1-C)^{(N-3)/2}}{N-2}\right.$$

$$+ \frac{N-1}{N}\,\frac{N-3}{N-2}\,\frac{(1-C)^{(N-5)/2}}{N-4} + \ldots + \frac{N-1}{N}\,\frac{N-3}{N-2}\,\frac{\cdots}{\cdots}\,\frac{5}{6}\,\frac{(1-C)^{3/2}}{4}$$

$$\left. + \frac{N-1}{N}\,\frac{N-3}{N-2}\,\frac{N-5}{N-4}\,\frac{\cdots}{\cdots}\,\frac{3}{4}\left[\frac{(1-C)^{1/2}}{2} + \frac{\sin^{-1} C^{1/2}}{2C^{1/2}}\right]\right.$$

$$- \frac{\sigma+1}{C^{\sigma/2}}\,\frac{\sigma}{2}\,\frac{(1-C)^{(N+1)/2}}{N+2} \qquad \text{(B-3a)}$$

The corresponding value for $\sigma = 1$ is

$$\mathrm{MI;\ EI} = \frac{2}{(N+1)C}\left[1 - (1-C)^{(N+1)/2}\right] \qquad \text{(B-3b)}$$

In the limit $C = 1$

$$\mathrm{MI;\ EI} = \frac{2}{N+1} \qquad (\sigma = 1) \qquad \text{(B-4a)}$$

$$= (\sigma+1)\left[1 - \frac{\sigma}{2}\,\frac{N+1}{N+2}\right]\left[\frac{N-1}{N}\,\frac{N-3}{N-2}\,\frac{\cdots}{\cdots}\,\frac{3}{4}\right]\frac{\pi}{4} \qquad (\sigma = 0,2) \qquad \text{(B-4b)}$$